Ilkogretim Online - Elementary Education Online, 2021; Vol 20 (Issue 5): pp. 5473-5484
http://ilkogretim-online.org
doi: 10.17051/ilkonline.2021.05.615

Bi-Faceted Binary Image Modernization Using Matrix Data Optimization Technique

Dr. Raman Chadha, Dean Engineering, Geeta Engineering College, Naultha Panipat, Haryana, India, dr.ramanchadha@gmail.com
Rajesh Kumar, Research Scholar, Career Point, Kota University, Rajasthan, rajesh0480@yahoo.com

Abstract- Image reconstruction is a method in which image data is reconstructed from input parcel data. The partial input data may include the horizontal projection, vertical projections, horizontal and vertical projections, diagonal projection, and anti-diagonal projection data. The image reconstruction algorithms are used to reconstruct the partially lost data or corrupted information as of the remaining traces of the image data. The binary image matrices are constructed of the 1-bit image pixels, which contains only two combinations and can hold the value of 1 and 0. The binary images are also classified as the black and white images, as two-bit images can only show either black or white color represented by 1 or 0 values in the binary image matrices. There are several binary image reconstruction methods already proposed for the binary image reform from some kind of input traces or the projection data to reconstruct the whole binary matrix. The initial image reconstruction solution is returned once the maximum iteration is reached or the horizontal and vertical combination different equals zero during the reconstruction by estimating the binary combinations produced by the projected mock-up solution. The heritable programming have been utilized in the second stage image matrix reconstruction, which utilizes the primary phases of image reconstruction based upon the genetic reproduction, which includes the crossover, mutation, and fitness for the finalization of the binary image matrix reconstruction solution. Various kind of experiments is being carried out through which a binary image can be reconstructed. Higher reconstruction accuracy has been recorded by the proposed model which is in the structure of the modernization fault. The time complexity has been evaluated in the proposed model evaluation against the existing models. The study talks about the proposed model for image reconstruction accuracy which has achieved a good position over the existing model.

Keywords: RGB, MATLAB,HV, OCR,CMYK.

I. INTRODUCTION OF IMAGE RECONSTRUCTION

The document introduction is based on image reconstruction and describes the process by which image data can be reproduced back by image traces [1]. The projection is the form through which traces of the image data can be obtained in a variety of dimensions. Image data is likely to help in getting horizontal, vertical, and diagonal projection [2] protrusion facts hold the addition of rows & columns which are in 2D and 3D form which depends on the type of images. The Binary images used in this paper are 1-bit images and are used only in two combinations which are 1 and 0. Binary Images reform depends on the initial solution, which computes the preliminary combination, which will satisfy the bulge data. Using protrusion data to redevelop the predictable dual images in an interactive framework and run the entire program itself. It has been formed by computing a variety of combinations to create initial image matrices. Matrix optimization is obtained through passing the matrix result which is obtained from an initial solution to the genetic algorithm. This is due to the projection data which was available with the best combination of an optimal solution for this G A will be responsible. This study will take into account a variety of parameters to examine the result and presentation score of the projected model. The parameters used are modernization accurateness, exactness, peak signal to racket ratio, forgotten time, and computational difficulty. There are a total of 5 components by which interactive image reconstruction algorithms will be created as shown below:

[1] An objective sculpt is an express the unfamiliar continuous-space meaning i.e. (f (r)) is to be rebuild in conditions of a limited series with unidentified coefficients that must be predictable from the information or data.

[2] A scheme sculpts that relate the unidentified entity to the "ideal" capacity that would be documented in the deficiency of amount blare. Frequently this is a linear sculpt of the outline (Ax + E), where E represent the sound.

[3] A geometric sculpt can be explain about the sound or noisy measurement which may be vary around their ideal values.

[4] The main effective is cost purpose i.e. to be minimized the image coefficient vector. Frequently this cost purpose includes some form of regularization. Occasionally the regularization is based on Markov random fields.

[5] The main algorithm used here is very iterative for reducing the cost function, which is including a number of images and a few stopping decisive factor for terminating the iterations.
The said Image may be defined as 2D function:
I = f(x,y)
Where x & y are the spatial coordinate. The strength (I) or else the gray value of the picture are label as the Amplitude (f) on any pair of coordinate i.e. value (x,y) shows. We can see that a digital picture is the term used for all the values of the spatial coordinator as well as amplitude are finite, discrete quantities.
Digital image processing may be later divided into several parts based on the method whose:

- Inputs along with outputs are images and
- There may be images that act as input and if it comes to output, it is an attribute that is extracted as of those images.

The image is formed including a variety of noises such as Gaussian sound or noise, speckle sound or noise, salt & pepper sound or noise, shot noise. Filtering is the foremost way to de-noising the image. The image that comes out is that it will either be blurred or smooth in excess because of the losses occurs in it.

1.1 Colour icon Processing

Person visual systems can differentiate a variety of shades and intensities in hundreds of thousands of dissimilar colors and, in grey color, only 100 shades are available. If the particular color has to illustrate, for that three independent quantity are used. It is the dominant wavelength through which *hue* is determined the electromagnetic spectrum if it is seen where the visible colors come from, it lies in between 400 mm (violet) and 700 mm (red). Excitation purity way to find out the saturation depends on the measure in which the white light is varied with hue. When it comes to pure hue, it is completely saturated, it also means that no white light is mixed inside it. Forgiven colors, hue, and the situation mutually find out the chromaticity. Ultimately, with the help of the actual amount of light, the intensity is determined, with lighter corresponding to more intense colors.

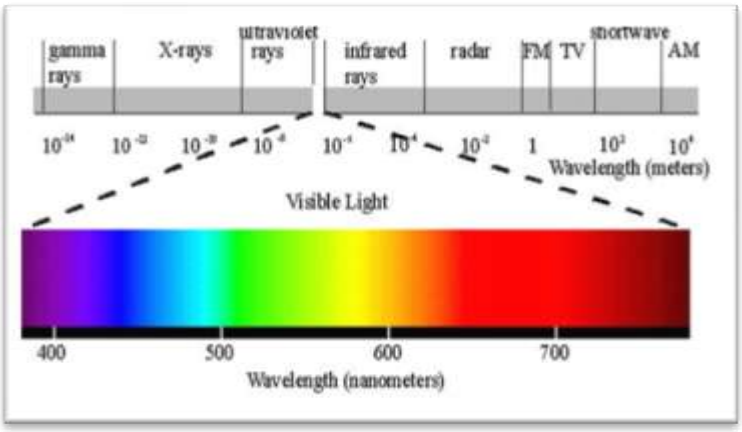

Figure 1.1 visible spectrum chart

1.2 Colour Perception

A total of three types of cone human retina have. Every type cone reaction works as a function of the wavelength of the confrontation light. The climax for every single curve is define as 440nm (i.e. in blue), 545nm (i.e. in green), & 580nm (i.e. red).

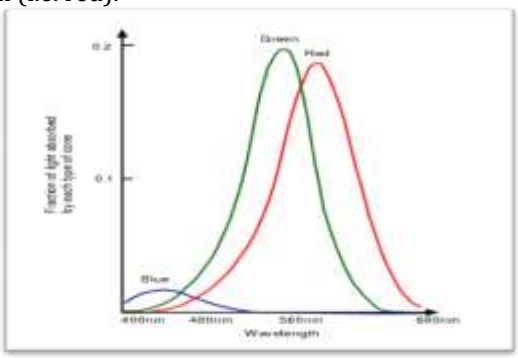

Figure 1.2. Climax value for every curve at 440nm (i.e. blue), 545nm (i.e. green), and 580nm (i.e. red).

1.3 Colour of Models

There are standard methods for specifying particular colors by color models. Which can be understood by the 3D coordinate system and subspace, which contains a particular model for all constructive colors? Any type of color can be particular as a sculpt will be in contact with a lone tip within the subspace.

1.4 The RGB(RED GREENBLUE) Model

Here Red Green and Blue i.e. RGB sculpt or model in every pics or image has three independent image planes; i.e. available in the primary color. Talking about primary colors, it's red, green, and blue. Now if each color has to be specified, it is important to specify the amount present in primary components.

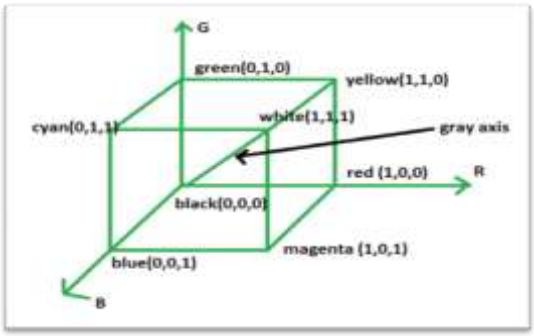

Figure 1.3 The color grayscale range lies join the vertices of black and white

1.5 The CMY/(Cyan-Magenta-Yellow) Model

The subtractive model which is suitable for the absorption of colors is known as the CMY (cyan-magenta-yellow) model. The example is that the pigments present in the paints. Here is given a relation that is between the RGB and CMY model which is:

$$\begin{bmatrix} C \\ M \\ Y \end{bmatrix} = \begin{bmatrix} 1 \\ 1 \\ 1 \end{bmatrix} - \begin{bmatrix} R \\ G \\ B \end{bmatrix}.$$

The mixing of three secondary colors is shown in **Figure 1.4**. It is made by mixing three primary colors which are red, green, and blue.

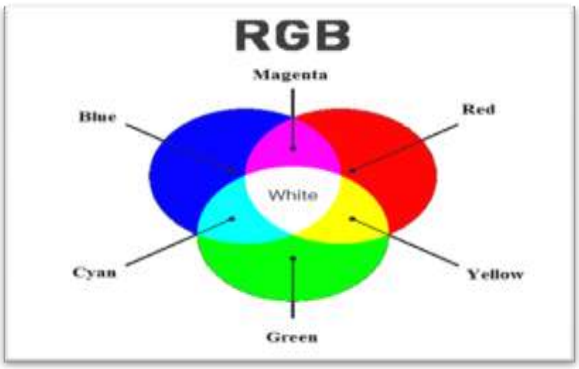

Figure1.4 RGB color model

Red and green are mixed to get yellow color, To get the cyan color the blue and green color is to be mixed. Combination of red, green, and blue to get the white color, at last, to get magenta color red and blue color is mixed through these mixing secondary colors is formed. Below it is explained in simple from.

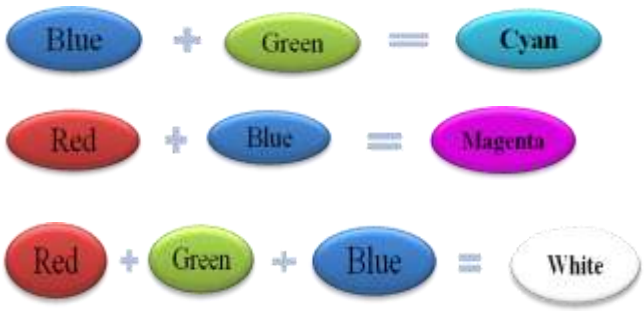

In above we can observe that CMY model is utilized in printing type all devices and the types of filters. We can observe in the Figure 1.5 shows three subtractive primaries and their pair wise combinations are indicated by which red, green, and blue colours can be retrieved, and finally, to obtain the white colour, the black colour will have to be subtracted from all the three primary colours.

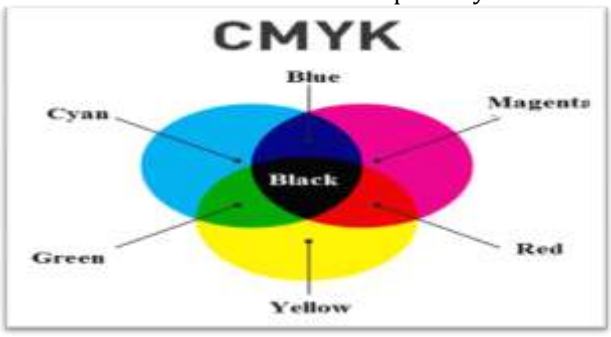

Figure 1.5 CMYK color model

II. PROBLEM FORMULATION

In this research paper, image reconstruction has been proposed over the binary images in the multi-level reconstruction. The binary image reconstruction in this research is based upon the horizontal and vertical (HV) projections. The HV-convex images are the images containing the multidimensional binary shapes in the binary matrix. The image reconstruction is useful for the reconstruction of the binary-based feature descriptor data, direct binary image captures, and OCR text extraction images. The proposed model is entirely aimed at solving the problem of the binary data recovery from the horizontal and vertical projections.

2.1 Research Objectives

i. To plan and evaluate the planned mold design to conquer the inadequacy of the obtainable model.
ii. To put into practice the initial solution generation with double-cross evaluation based upon segmentation.
iii. The MATLAB simulator has to be used for the proposed model for its implementation and debug.
iv. To obtain and analyze the results from the proposed model design.
v. To shortlisted the image de-noising filters would be analyzed for their performance.
vi. To find the shortcomings of the existing image de-noising filters
vii. To design the improved median filter algorithm or hybridized picture de-noising filter
viii. To implement the newly designed improved median filter algorithm or hybridized image de-noising filter
ix. In the direction of obtaining results of the newly proposed picture de-noising filter

2.2 Formulation

The model presented in this study has been created for the image rebuilding solution generation using double-level (Optimization Problem 1 and 2) along with the simulated annealing algorithm. The simulated annealing algorithm inherits the idea of metallurgy where this method is applied over the metal or glass to cool it slowly to remove the internal stress and toughen the metal or glass. The annealing gives the best strength in the metal or glass with appropriate flexibility. The solution is hence applied over the HV-convex image regeneration, where it has been applied to resolve the problem of 2-D binary matrix reconstruction to create a robust solution for image reconstruction. But the simulated annealing may not

act as the appropriate solution over the binary image matrix, as there is quite a high probability of creating the error during the image reconstruction as defined in the exiting scheme results. Also, the solutions for the optimization problems 1 and 2 may mess up each other while applied in a layered fashion. A single robust initial solution creation algorithm will produce more accurate and robust solutions.

There different types of sounds or noises are shaped in the figure data. The research in this study emphasizes to remove the salt & paper effectively from the image without quality degradation.

It causes a lot of impact on the image if a hide the detail which is present in the image, and it also makes a difference in the clarity of the images. Usually, when transferring the file we are faced with salt and paper noise. This noise has a total of two possible values are 0 and 1. The probability of each value is less than 0.

III. DESIGN AND IMPLEMENTATION

In general, the solution space of the reconstruction problem is very large [99]. Thus to get solution one requires some constraints. do not provide a unique solution, making it natural to select some optimal (concerning some pre-defined optimality criterion, according to the application area) solution.

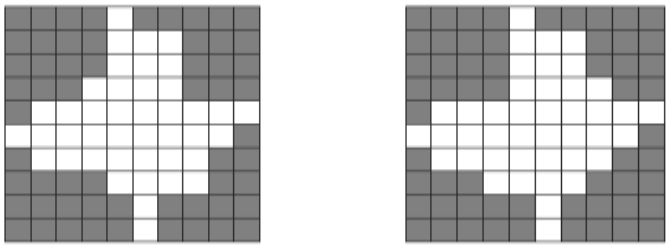

Figure 3.1: Two different HV- convex images with the same projection set

In this chapter, the convexity constraint is used to minimize the solution space. The class of **HV** convex binary images has been considered, as the solution space for a given set of projections, the projection set with two orthogonal directions namely, horizontal(1, 0) and vertical direction (0,1) only has been taken. Thus we have the projection set $P(R, C)$, $R = \{r_1, r_2, \ldots . r_m\}$, and $C = \{c_1, c_2, \ldots . c_n\}$. The HV convexity with projections from two directions does not provide a unique solution [12].

In practical applications the class of h-v convex matrices with given projections in two directions $v_1 = (1, 0)$ and $v_2 = (0, 1)$ is very large, making it impossible to find the exact solution [64]. Moreover many times the exact solution is not required (for example, it may add instrumentation error in projections to the solution), thus the most favorable way out in the sought after solution in such problems. Because the class is large and the optimization criteria are depending on only projection data and a-priori information usual optimization methods may not work well, hence stochastic optimization technique (minimization algorithm) known as Genetic programming derived from thermodynamics [129,149] is used here. The study is also focused on the challenges and use of big data in [15]. In section 3.2 we will give a brief description of Genetic programming approach, in section 3.3 analog of Genetic programming in discrete tomography is described, section 3.4 gives the brief description of boundary point and envelop points, section 3.5 gives the proposed reconstruction algorithm based on Genetic programming approach, in section 3.6 implementation of proposed reconstruction algorithms is given, in section 3.7 investigational outcome of the proposed algorithm are shown, and in segment 3.8 conclusion of the proposed algorithms is given. A novel multi-focus image fusion paradigm: a hybrid approach [16]. The research is based on also latest trends on heart disease prediction using machine learning and image fusion [17].

3.1 Genetic Programming

Genetic programming is a global optimization algorithm in the class of stochastic optimization algorithms and Meta-Heuristic algorithms. Genetic programming is an adaption of biological chromosomal selection and is used in function optimization. This approach gives a basis for a large variety of extensions and specifications of the general method.

Genetic programming is encouraged through the process selection in genetics in natural creation. In this natural process of the gene theory associated with the genome production in biological entities such as humans, etc In this process the chromosome sets of 23 chromosomes each are obtained from the female and male components, which undergoes the selection of the fittest 23 chromosomes for the new population.

3.2 Genetic Programming Approach In Discrete Tomography

The analogy of this physical process of offspring production in the biological entities becomes very important for the survival of the genomes. To complete the population generation process through gene theory, the projected model has been proposed to create the image by using a similar mechanism to the biological offspring production.

The chromosomes $(i,j) \in X$ are the state variables in the system, which is to be reached at genetic equilibrium at the optimal biological conditions and situations, this is represented as each image has a given projection set and/or some a-prior information is also to be satisfied. By slow cooling, the system can be optimized in the minimum rotations or iterations, which is the minimization of some cost (fitness) function. In other words, Genetic programming based approach can be defined as:

For a given projection set P and constraints, define the class $\mathcal{F}$ of possible solutions, this class is the search space. Each element F of search space $\mathcal{F}$ is a binary image containing (mn) values (pixels/cells f_{ij} f_{ij}) which are conditions (variables), the new generation production process says that the values of f_{ij} f_{ij} can be interchanged such that $F \in \mathcal{F}$ $F \in \mathcal{F}$ (select of optimal chromosomes), cooling will say to find such F F which lowers the energy (cost/ fitness function) by selecting the optimal pairs ought to reach an optimal or near-optimal solution.

In this Genetic programming procedure, the selection of chromosomes is taken as switching operation, the switching operation as a free movement has been considered in this thesis to take the binary bit decisions based on the environmental conditions or variables calculated during the various iterations. In present work the switching is carried on only at the boundary of the image since the number of pixels (cells) on the boundary is in a smaller amount than the number of pixels (cells) in the entire image, this will speed up the complete process.

3.3 Adjacent Points, Boundary Points and Envelop Points

In this section, some definition is given which explain the movement of chromosomes in Genetic programming process.

3.3.1 Adjacent cells and adjacent points

Any two cells (i,j) (i,j) and (i',j') (i',j') in X is said to be adjacent if either $i = i$ $i = i$ and $|j-j'| = 1$ $|j-j'| = 1$ or $|i-i'| = 1$ $|i-i'| = 1$ and $j = j'$ $j = j'$. **3.3.2 Adjacent points of a binary image or connected image**

If $f_{ij} = F(X(i,j))$ $f_{ij} = F(X(i,j))$ and $f_{i'j'} = F(X(i',j'))$ $f_{i'j'} = F(X(i',j'))$ both have value 1 and cells (i,j), (i,j), and (i',j') (i',j') are adjacent then these points of binary image are said to be connected. If all the points of binary image F are connected then it is called connected image.

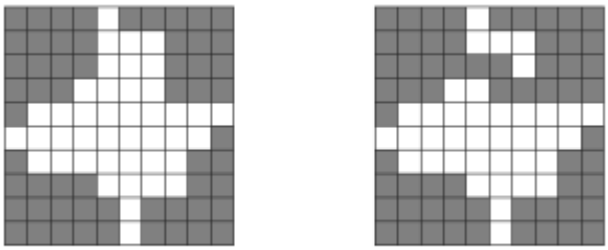

Figure 3.2: Connected binary image and not connected binary image

3.3.3 Boundary of a binary image

The binary image F F says that it contains 1's at some cell (i, j) and 0's at other cells in the discrete set X X, hereafter by an image we will refer the cells having a value of F F as 1 i.e $F(X(i,j)) = f_{ij} = 1$ $F(X(i,j)) = f_{ij} = 1$ and the cell or point (I,j) of X will be said to be a point of binary image F F, i.e. $f_{ij} = 1 \Longrightarrow (i,j) \in F$ $f_{ij} = 1 \Longrightarrow (i,j) \in F$.

The set of all cells (points) (i, j) in F F which separate 1's from 0's will be called the boundary of F F, thus the boundary of F F is represented as

$B_F = \{(i,j) \in F : \exists\ adjacent\ point\ (i',j') \notin F\}$ $B_F = \{(i,j) \in F : \exists\ adjacent\ point\ (i',j') \notin F\}$ (3.1)

Similarly, the boundary is defined in [202].

3.3.4 Boundary point

The element $(i,j) \in B_F$ $(i,j) \in B_F$ will be called the boundary point. Thus boundary point can be defined alternatively: A point (cell) $(i,j) \in F$ $(i,j) \in F$ will be called boundary point if at least one of the following four properties is satisfied

(i) $f_{i-1,j} = 0 \; or \; i = 1$ $f_{i-1,j} = 0 \; or \; i = 1$

(ii) $f_{i,j-1} = 0 \; or \; j = 1$ $f_{i,j-1} = 0 \; or \; j = 1$

(iii) $f_{i+1,j} = 0 \; or \; i = m$ $f_{i+1,j} = 0 \; or \; i = m$

(iv) $f_{i,j+1} = 0 \; or \; i = n$ $f_{i,j+1} = 0 \; or \; i = n$

Based on this alternative definition boundary points can be categorized in the following categories:
If a boundary point satisfies only one property it will be called type 1 boundary point, if any boundary point satisfies any two properties only it will be called type 2 boundary points, if any boundary point satisfies any 3 properties only then it will be called type 3 boundary points. A boundary point satisfying all four properties will be an isolated point of the image F F and will be called type 4 boundary points.

3.3.5 Inner point

A cell (point) $(i,j) \in F$ $(i,j) \in F$ will be the inner point of the binary image if it is not the boundary point. Thus the inner point is a point $(i,j) \in F \quad and \; (i,j) \notin$ $(i,j) \in F \quad and \; (i,j) \notin$ B_F B_F.

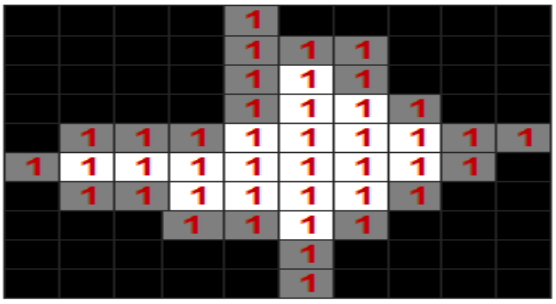

Figure 3.3: Boundary points and inner points

3.3.6 Envelop and envelop points of binary image F F

The set of all cells (points) in X X but not in F F, which separate 1's of F F from 0's is called the envelop of F F.

$E_F = \{(i,j) \notin F : \exists \; adjacent \; point \; (i,j) \in F\}$

$E_F = \{(i,j) \notin F : \exists \; adjacent \; point \; (i,j) \in F\}$ (3.2)

And element $(i',j') \in E_F$ $(i',j') \in E_F$ will be called the envelop point. Thus envelop point can be defined alternatively as a point (cell) $(i',j') \notin F$ $(i',j') \notin F$ i.e. $f_{i,j} = 0$ $f_{i,j} = 0$ will be called envelop point if at least one of the following four properties is satisfied

(i) $f_{i-1,j} = 1$ $f_{i-1,j} = 1$

(ii) $f_{i,j-1} = 1$ $f_{i,j-1} = 1$

(iii) $f_{i+1,j} = 1$ $f_{i+1,j} = 1$

(iv) $f_{i,j+1} = 1$ $f_{i,j+1} = 1$

Based on this alternative definition envelop points can be categorized as:
If a envelop point satisfies only one property it will be called type 1 envelop point, if any envelop point satisfies any two properties only it will be called type 2 envelop point, if any envelop point satisfies any 3 properties only then it will be called type 3 envelop point. A envelop point satisfying all four properties will be a hole of image F and will be called type 4 envelop point.

Figure 3.4: Boundary points, envelope points, and inner points

3.3.7 Boundary point switching

The given projection set has a projection in two directions namely horizontal and vertical, so the switching component will contain only four points (cells) in X. If the elements of the switching component are adjacent, then it will be called the boundary point switching component.

Let the two disjoint subsets I_1 I_1 and I_2 I_2 of switching component $I_1 \cup I_2$ $I_1 \cup I_2$ are $I_1 = \{(i_1,j_1)\ (i_2,j_2)\}$ $I_1 = \{(i_1,j_1)\ (i_2,j_2)\}$ and $I_2 = \{(i_1,j_2)\ (i_2,j_1)\}$ $I_2 = \{(i_1,j_2)\ (i_2,j_1)\}$

if $I_1 \subset B_F$ $I_1 \subset B_F$ ($I_1 \subset E_F$) $I_1 \subset E_F$) and $I_2 \subset E_F$ $I_2 \subset E_F$ ($I_2 \subset B_F$ $I_2 \subset B_F$ respectively) then this switching operation with this kind of switching component is called boundary point switching.

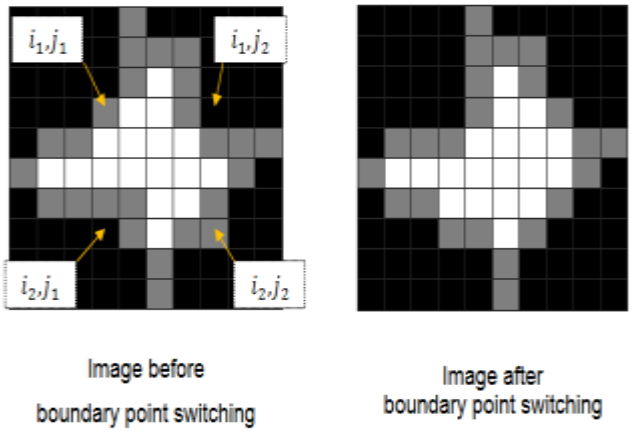

Figure 4.5: Boundary point switching component and switching result

3.3.8 Measure of convexity

Let n_h (respectively n_v) denote all horizontally (respectively vertically) adjacent cells in F F, n_h (respectively n_v) can be used as a measure of horizontal (respectively vertical) convexity.

Let n_h denote all horizontally adjacent cells in F F, also n_h can be used as a measure of horizontal convexity, similarly, n_v may be considered for vertical convexity denoting all vertical adjacent cells in F F.

Thus for the binary image $F = (f_{ij})_{m\times n}$ $F = (f_{ij})_{m\times n}$ having projection set $\mathcal{P}(R,C)$ $\mathcal{P}(R,C)$ with $R = \{r_1, r_2, \ldots . r_m\}$ $R = \{r_1, r_2, \ldots . r_m\}$ $C = \{c_1, c_2, \ldots . c_n\}$ $C = \{c_1, c_2, \ldots . c_n\}$

$n_h = \sum_{i=1}^{m} \sum_{i=1}^{n-1} f_{ii} f_{ii+1}$ $n_h = \sum_{i=1}^{m} \sum_{i=1}^{n-1} f_{ii} f_{ii+1}$ (3.3)

and

$n_v = \sum_{i=1}^{n} \sum_{i=1}^{m-1} f_{ii} f_{i+1i}$ $n_v = \sum_{i=1}^{n} \sum_{i=1}^{m-1} f_{ii} f_{i+1i}$ (3.4)

Let us define a measure for *hv*-convexity as

$n_{hv} = n_h + n_v$ $n_{hv} = n_h + n_v$ = number of horizontally and vertically adjacent cells in F F, so

$n_{hv} = \rangle\ \rangle\ f_{ii} f_{ii+1} + \rangle\ \rangle\ f_{ii} f_{i+1i}$ (3.5)

it may be noted that

$n_h \leq \sum_{i=1}^{m} (r_i - m)$ $n_h \leq \sum_{i=1}^{m} (r_i - m)$ (3.6)

where r_i r_i is the i[th] horizontal projection set $\mathcal{P}$ $\mathcal{P}$(R, C). Since the number of adjacent cells in the i[th] row F F will always be less than or equal to the number of 1's in i[th] row of F F. If the image is h-convex then

$n_h = \sum_{i=1}^{m} (r_i - m)$ $n_h = \sum_{i=1}^{m} (r_i - m)$ (3.7)

Similarly

$n_v \leq \sum_{i=1}^{m}(c_i - n)$ $n_v \leq \sum_{i=1}^{m}(c_i - n)$ (3.8)

and if the image is v-convex, then

$n_v = \sum_{i=1}^{m}(c_i - n)$ $n_v = \sum_{i=1}^{m}(c_i - n)$ (3.9)

Thus

$n_{hv} = n_h + n_v \leq \sum_{i=1}^{m}(r_i - m) + \sum_{i=1}^{n}(c_i - n)$

$n_{hv} = n_h + n_v \leq \sum_{i=1}^{m}(r_i - m) + \sum_{i=1}^{n}(c_i - n)$ (3.10)

Since the projection set $\mathcal{P}(R, C)$ $\mathcal{P}(R, C)$ has to be compatible with the reconstruction problem. Thus $\sum_{i=1}^{m} r_i = \sum_{i=1}^{n} c_i = N$ $\sum_{i=1}^{m} r_i = \sum_{i=1}^{n} c_i = N$ = total number of cells in F F.

Hence

$n_{hv} \leq 2\sum_{i=1}^{m}(r_i - m - n) = \sum_{i=1}^{n}(c_i - m - n)$

$n_{hv} \leq 2\sum_{i=1}^{m}(r_i - m - n) = \sum_{i=1}^{n}(c_i - m - n)$ (3.11)

And if the image is *hv* convex then

$n_{hv} = 2\sum(r_i - m - n) = \sum(c_i - m - n) = 2N - (m + n)$ (3.12)

Thus for the reconstruction of *hv* convex images, the fitness (cost) function should be to achieve convexity, thus here the optimality criterion has been considered to maximize

$n_{hv} = 2\sum_{i=1}^{m} r_i - (m + n)$ $n_{hv} = 2\sum_{i=1}^{m} r_i - (m + n)$ (3.12)

3.4 RECONSTRUCTION ALGORITHM BASED ON GENETIC PROGRAMMING

Our reconstruction problem $(F_{hv}, \mathcal{P})$ $(F_{hv}, \mathcal{P})$ $\mathcal{P} = P(R, C)$ $\mathcal{P} = P(R, C)$ has been transformed into an optimization problem

$\max(n_{hv})$ $\max(n_{hv})$ (3.13)

Subject to

$\sum_{i=1}^{m} f_{ij} = c_j \quad \forall j = 1(1)n$ $\sum_{i=1}^{m} f_{ij} = c_j \quad \forall j = 1(1)n$ (3.14)

The proposed reconstruction algorithm based on Genetic programming approach:

3.4.1 Initial solution

The initial solution of reconstruction (G_{bg}, HV) (G_{bg}, HV) is obtained using any basic reconstruction algorithm, which does not provide the *hv* convex image.

3.4.2 Image regeneration process

The boundary point switching operation has been considered the free selection of chromosomes, so the chromosomes are boundary point switching components. At the highest probability, which is the starting point, all boundary points switching components have equal probability to be chosen, as the probability goes down, the fitness is controlled with changing the assignment of the probability of boundary point switching components to be chosen for switching operation. The assignments of probabilities to these switching components have been done according to the category of boundary points and envelop points taken together in the switching component. In our algorithm, it has been assigned a higher value to a boundary point switching component, if the possibility of improvement in a measure of convexity is higher.

Thus, in a typical iteration the boundary point switching operation is performed on all those switching components which have been assigned the highest probability, and at that probability (per iteration) solution is obtained. In the next iteration, again the boundary points, envelop point and boundary point switching components in a new obtained solution will be identified and another assignment of probability is done according to the category of boundary points and envelop points.

3.4.3 Termination

The fittest solution is achieved when we stop the iterations. The stopping criteria have been taken as when either change in assignment of probabilities to the switching components is not significant (not possible) or the change in assignment of probabilities does provide the possibility to change in the measurement of convexity (or in the value of cost/fitness function), whichever is achieved earlier.

3.5 Implementation of Reconstruction Algorithm

The proposed reconstruction algorithm is implemented as

Step 1: Get initial solution F F^0 using algorithm 2.7.2 and set tm := Maxt and niter:=1

Step 2: Find B_F the set of boundary points and E_F set of envelope points of F .

Step 3: If niter > tm then exit

Step 4: For each element of B_F find all boundary point switching components and according to their category assign the probability as the highest probability to switching component have isolated point or type 4 boundary points. And in order of the type of boundary point assign the probability to all switching components.

Step 5: Perform the switching operation on switching components with maximum probability in F F

Step 6: set niter = niter + 1. If the value of cost function N_{hv} is improved then Go to step 2 and set tm = niter + maxt. Else Go to step 4 and choose another component in B_F with the next highest probability to perform switching operation and increase.
Step 7: Repeat steps 2 to 6 until improvement n_{hv} n_{hv} is significant.

IV. RESULT ANALYSIS

For experimental study the test set of convex binary images of sizes 100,400, 900, 1600, 2500, 3600, 4900, 6400, 8100 are generated, for each size a set of 100 images has been generated. For each image, the horizontal and vertical projections are calculated as row sum and column sum of corresponding binary matrices. Thus an image of size nxn will have projection set $\mathcal{P}$ $\mathcal{P}$(R, C) with $R = \{r_1, r_2, \dots, r_m\}$ $R = \{r_1, r_2, \dots, r_m\}$, $C = \{c_1, c_2, \dots, c_n\}$ $C = \{c_1, c_2, \dots, c_n\}$. A characteristic instance of a dual image of size 400(20x20) and its protrusion set $\mathcal{P}$ $\mathcal{P}$(R, C) are specified in figure 5.1.

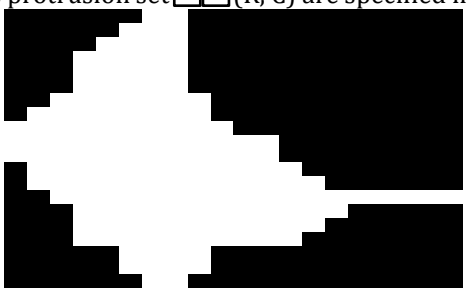

Figure 5.1: Image 20x20 and its Projection Set

R = {2,3,4,5, 5, 5, 7, 8, 10, 12, 12, 12, 13, 18, 12, 11, 10, 4, 4, 2}

C =
{3,6, 8, 14, 15, 18, 20, 20,
13, 9, 8, 8, 6, 4, 2, 1, 1, 1, 1, 1}

C =
{3,6, 8, 14, 15, 18, 20, 20,
13, 9, 8, 8, 6, 4, 2, 1, 1, 1, 1, 1}

On these image sets we implemented the proposed reconstruction algorithm 5.6.1; we also implemented the algorithm given in on these images. The performance of these algorithms is compared with the measure of convexity defined in section 5.5.8 and the reconstruction error defined as normalized L_1 error given in following

$$E_R = |F - \bar{F}| = \text{—— } \rangle \rangle |f_{ij} - f_{ij}| \qquad (5.5.3)$$

Where F F and $\bar{F}$ $\bar{F}$ are the original image and reconstructed images respectively. In fig 5.1 the measure of convexity for reconstructed typical image of each size is given as shown in equation (5.5.1), the bound is the maximum value of convexity measure n_{hv} n_{hv} as shown in equation (5.5.2).
The average value of n_{hv} n_{hv} and average reconstruction error (E_R E_R) for different sizes of images ranging from 10x10 to 100x100 are reported. The average is taken on a complete set of 100 images in each size. The convergence of both algorithms concerning the convexity measure n_{hv} n_{hv} is reported for a typical image of size 40 x 40. It is experiential that the algorithm converges faster than the algorithm. Further to test the stability of algorithm we added discrete uniform random noise in calculated projections and the reconstruction by these algorithms is obtained using these noisy projections. For adding noise in projection data, we generated discrete uniform random number from {-k, -k+1, …, -1, 0, 1, …, k-1, k} for k=1, 2, 3, 4 and 5. These are referred here as 1%, 2%, 3%, 4% and 5% noise in projection data.
The convergence of our algorithm 5.6.1 and the algorithm [jerry] with noisy projection data concerning convexity measure n_{hv} n_{hv} for a typical image of size 40x40 are reported in table 5.5 to table 5.9 and their graphical representations are given in figure 5.9 to 5.13. Further, the average n_{hv} n_{hv} and average E_R E_R in the reconstruction of each size of images with noisy projections are reported. The convexity of the algorithm has been image after the application of the reconstruction solution.

V. CONCLUSION

The image reconstruction is the practice to produce the image as of the projection data. There are numerous type of protrusion information or data, which can be obtained as of the input image matrix. Mainly the image projection data is obtain in the form of flat, perpendicular, horizontal-vertical, slanting, and anti-diagonal projections from the input image matrix. The binary image matrix has been obtained from the various applications, which are used in this image matrix reconstruction practice. The figure matrix rebuilding method used for the planned model which is based on two things, the chang's algorithm and the hereditary algorithm. The genetic algorithm is processed over the post matrix for final stage recovery. Talking about a genetic algorithm, it is an optimization algorithm based upon fundamentals of the inherited duplicate. The main factors or functions that are designed by combining crossover mutations and new population production are the function through which it is formed. Genetic algorithms are used in a variety of computer applications where optimization is also required. The proposed model is tested with a variety of binary images with image size lies between 10*10 and 100*100.In the results assessment, whatever experiments have been made in this study are shown in the tabular form and it shows results that have been made from the various rounds experiments on the reconstruction of the image. The study has achieved experimental results in the formation of the time complexity & reconstruction an error. In the existing body, the modernization error recorded is much lower as compared to the proposed model. Recorded with roughly 80% difference. This is a huge development in the post model.

VI. FUTURE SCOPE

There is a chance of progress of the proposed model later on for the time unpredictability. It tends to be planned rapidly by the hereditary calculation model. Additionally, the preferred model over the hereditary calculation can be delivered.

REFERENCES

[1] Patel, Divyesh, and Tanuja Srivastava. "Reconstructing h-convex binary images from its horizontal and vertical projections by simulated annealing." In *Contemporary Computing (IC3), 2015 Eighth International Conference on*, pp. 117-121. IEEE, 2015.

[2] Verma, Shiv Kumar, Tanuja Shrivastava, and Divyesh Patel. "Efficient Approach for Reconstruction of Convex Binary Images Branch and Bound Method." In *Proceedings of the Third International Conference on Soft Computing for Problem Solving*, pp. 183-193. Springer India, 2014.

[3] Nagy, Ábris, and Csaba Vincze. "Reconstruction of hv-convex sets by their coordinate X-ray functions." *Journal of mathematical imaging and vision* 49, no. 3 (2014): 569-582.

[4] Srivastava, Tanuja, Shiv Kumar Verma, and Divyesh Patel. "Reconstruction of binary images from two orthogonal projections." *IJTS* 21, no. 2 (2012): 105-114.

[5] Mohamed, Hadded, and Hasni Hamadi. "Combining Genetic Algorithm and Simulated Annealing Methods for Reconstructing HV-Convex Binary Matrices." In *Hybrid Metaheuristics*, pp. 78-91. Springer Berlin Heidelberg, 2013.

[6] Hantos, Norbert, and Péter Balázs. "A uniqueness result for reconstructing hv-convex polyominoes from horizontal and vertical projections and morphological skeleton." In *Image and Signal Processing and Analysis (ISPA), 2013 8th International Symposium on*, pp. 795-800. IEEE, 2013.

[7] Ozsvár, Zoltán, and Péter Balázs. "An Empirical Study of Reconstructing hv-Convex Binary Matrices from Horizontal and Vertical Projections." *Acta Cybern.* 21, no. 1 (2013): 149-163.

[8] Patel, Divyesh, and Tanuja Srivastava. "Reconstruction of binary matrices satisfying neighborhood constraints by simulated annealing." *World Academy of Science, Engineering and Technology* 8, no. 5 (2014): 760-763.

[9] Hantos, Norbert, and Péter Balázs. "A Fast Algorithm for Reconstructing hv-Convex Binary Images from Their Horizontal Projection." In *Advances in Visual Computing*, pp. 789-798. Springer International Publishing, 2014.

[10] Kashuk, Sina, and Magued Iskander. "Reconstruction of three dimensional convex zones using images at model boundaries." *Computers & Geosciences* 78 (2015): 96-109.

[11] Moscariello, Antonio, Richard AP Takx, U. Joseph Schoepf, Matthias Renker, Peter L. Zwerner, Terrence X. O'Brien, Thomas Allmendinger et al. "Coronary CT angiography: image quality, diagnostic accuracy, and potential for radiation dose reduction using a novel iterative image

reconstruction technique—comparison with traditional filtered back projection." *European radiology* 21, no. 10 (2011): 2130-2138.
[12] Leipsic, Jonathon, Giang Nguyen, Jaqueline Brown, Don Sin, and John R. Mayo. "A prospective evaluation of dose reduction and image quality in chest CT using adaptive statistical iterative reconstruction." *American Journal of Roentgenology* 195, no. 5 (2010): 1095-1099.
[13] Pontana, François, Alain Duhamel, Julien Pagniez, Thomas Flohr, Jean-Baptiste Faivre, Anne-Lise Hachulla, Jacques Remy, and Martine Remy-Jardin. "Chest computed tomography using iterative reconstruction vs filtered back projection (Part 2): image quality of low-dose CT examinations in 80 patients." *European radiology* 21, no. 3 (2011): 636-643.
[14] Ravishankar, Saiprasad, and Yoram Bresler. "MR image reconstruction from highly undersampled k-space data by dictionary learning." *Medical Imaging, IEEE Transactions on* 30, no. 5 (2011): 1028-1041.
[15] Khan, M., et al. (2020). Big Data and Social Media Analytics: A Challenging Approach in Processing of Big Data. Springer, Singapore. https://doi.org/10.1007/978-981-15-7961-5_59
[16] Muskan Jindal; Eshan Bajal; Alakananda Chakraborty; Prabhishek Singh, Ph.D; Manoj Diwakar; Neeraj Kumar, "A Novel Multi-Focus Image Fusion Paradigm: A Hybrid Approach", Materials Today: Proceedings,Elsevier, 2020.
[17] Manoj Diwakar, Amrendra Tripathi, Kapil Joshi, Minakshi Memoria , Prabhishek Singh, Neeraj kumar, "Latest Trends on Heart Disease Prediction using Machine Learning and Image Fusion", Materials Today: Proceedings,Elsevier, 2020.